A high-order approximate-mass spline collocation scheme for incompressible flow simulations

By Olivier Botella

1. Motivation and objectives

The development of numerical methods based on B-spline methodology is motivated by the substantial computational cost of large-eddy simulations (LES) of complex turbulent flows. Indeed, the large number of grid points needed in turbulent boundary layers remains one of the principle obstacles to a wider application of LES to flows of engineering interest. An active part of research in LES is devoted to reducing these resolution requirements by the formulation of approximate wall conditions (see *e.g.* Nicoud *et al.* (2001)) and by the development of highly accurate numerical methods for the precise representation of near-wall structures.

Several works (Shariff & Moser (1998); Kravchenko *et al.* (1999); Kravchenko & Moin (2000)) have been devoted to the development of B-spline methods on semi-structured embedded meshes. This technique allows a substantial reduction in the computational cost of a simulation by using fine grids in physically significant flow regions only. The use of B-splines is motivated by the development of robust and non-dissipative LES schemes on arbitrary meshes. The conservation of physical invariants such as kinetic energy is highly desirable for the simulation of turbulent flows (Kravchenko & Moin (1997)), and these requirements are difficultly reproduced by finite-difference schemes on non-uniform meshes (Vasilyev (2000)). Moreover, the resolution power of B-splines of maximum continuity allows the representation of a broad range of scales of a turbulent flow (Kravchenko *et al.* (1999)).

The work of Kravchenko *et al.* (1999) and Kravchenko & Moin (2000) has shown the high suitability of B-spline methods for the computation of complex turbulent flows. However, the Galerkin approximation that is employed is too CPU intensive. The method is burdened by the cost of evaluating nonlinear terms where, as observed in Kravchenko *et al.* (1999), 50% of the computational time is spent on their evaluation.

This report represents a follow-up to the work initiated in Botella (1999, 2001) for developing a cost-effective B-spline Navier-Stokes solver. The equations are discretized with the collocation method, which allows a drastic reduction of the cost of evaluating nonlinearities. A stable approximation of the pressure is obtained by constructing staggered bases for the velocity and pressure which are, in a sense, the B-spline equivalent to the popular staggered finite-difference discretization (Harlow & Welch (1965)). The time-discretization employs a fractional step scheme.

In association with "local" (or "explicit") discretizations such as finite-difference or finite-volume approaches, fractional step techniques are widely considered as the most cost-effective method for solving the Navier-Stokes equations. Indeed, they provide a maximum decoupling of the velocity and the pressure so that only sparse elliptic problems need to be solved at each time-cycle. However, for "global" discretizations such as B-spline methods that yield a non-diagonal mass matrix, a straightforward application of these methods retains some coupling between the velocity and pressure: the pressure

operator associated with the projection step, which involves the dense inverse of the mass matrix, is dense and can only be constructed for modestly sized problems. As suggested in Botella (1999, 2001), the pressure equation can nonetheless be solved by means of a Uzawa algorithm, but the CPU cost of this iterative solution, even accelerated by modern Krylov subspace methods (Saad (1996)), is prohibitively high for large scale problems.

In order to make this B-spline method attractive with respect to CPU cost, we have made an effort to modify the fractional step scheme in order to obtain a simpler linear system for the pressure that would be sparse and to eliminate the need for Uzawa iterations. A modification of the mass matrix to get a sparse approximation of its inverse is a key element in this endeavor.

The modification of the "consistent approximation", which generates the non-diagonal mass matrix, has always been a critical issue for finite-element type methods. A common *ad hoc* simplification consists in approximating the mass matrix by a diagonal matrix, usually by summing its rows and putting the result on the diagonal (the "lumped mass" approximation, see *e.g.* Gresho & Sani (1998)). For compressible flow simulations, this simplification is motivated by the use of explicit time-stepping such that, when the time-derivative term is lumped, the inversion of the consistent mass matrix is no longer needed at each time cycle. This mass lumping technique, however, diminishes the accuracy of the resulting scheme, most notably for unsteady flows dominated by convection effects (Gresho *et al.* (1978)), since this approximation is, in general, a first-order approximation of the consistent mass matrix.

So far, the most satisfying application of the lumping technique to incompressible flow computations is represented by the "projection 2" scheme of Gresho & Chan (1990). It uses a semi-consistent mass matrix approximation (SCM), *i.e.* the mass matrix is lumped in front of the pressure gradient only, while the continuity equation is unaltered. As a consequence, the pressure operator is sparse and can be efficiently inverted by standard elliptic solvers. Early applications of the SCM technique to the B-spline collocation method were reported in Botella (1999, 2001). For low-order spline approximations, this scheme performed accurate Navier-Stokes benchmark computations with only a fraction of the CPU time needed by the original consistent scheme. However, due to the crude approximation represented by the lumping of the mass matrix, the SCM scheme led to a loss of the accuracy that would be expected for high-order B-splines.

In order to preserve as far as possible the high accuracy of the B-spline method, it is thus necessary to build more accurate approximations of the consistent mass matrix than the lumped approximation. These considerations led us in this work to the development of approximate inverses of the mass matrix, *i.e.* highly-accurate sparse approximations of the inverse of the consistent mass matrix. This concept of approximate inverse is somewhat similar to the one developed for the iterative solution of linear systems, where the approximate inverse is an explicit preconditioner whose application in an iterative procedure requires a sparse matrix-vector multiplication only (see *e.g.* Saad (1996)). The main difference is that we are able to replace the solution of a mass matrix problem by a single sparse matrix-vector multiplication while keeping the order of accuracy of the B-splines.

For the B-spline collocation method, such sparse approximations are obtained by application of local interpolation schemes. These schemes of quasi-interpolation were developed in *e.g.* Lyche & Schumaker (1975); de Boor (1978) to build spline representation of a function from data values. The B-spline coefficients are not determined as the solution to a collocation system, as the consistent approximation would require, but rather as the

linear combination of the function values at a small number of data points. When these data points are chosen among the collocation points, this linear combination defines the entries of the approximate inverse of the mass matrix. The number of data points affects the order of accuracy of the approximate inverse. The case with a single data point corresponds to the low-order lumped approximation. The increase in the number of data points raises the order, and a sufficient number of points yields the order of accuracy of the consistent approximation. These approximate inverses thus represent a high-order generalization of the mass lumping technique.

The concepts of approximate inverse and local interpolation may have important application to numerical algorithms where a fast transformation from the physical (collocation) space to the B-spline coefficients space is required. Among others, we cite the development of restriction operators for spline multigrid methods (Christara & Smith (1997)) and the evaluation of nonlinearities in collocation space, as in the pseudospectral method. In this report, the use of an approximate inverse allows us to solve the pressure equation of the Navier-Stokes scheme with a fraction of the CPU time required by the consistent approximation, with the same order of accuracy. The slight loss of the resolving power of the semi-consistent schemes, caused by the replacement of the consistent mass matrix, is greatly counterbalanced by their computational efficiency. These issues are carefully addressed here by presenting numerical tests and Fourier analysis. The combination of these approximate inverses with the SCM fractional-step technique allows the construction of a highly-accurate cost-effective Navier-Stokes solver, as proved by the benchmark tests reported in this paper.

2. Background on B-spline numerical schemes

2.1. *Construction of B-spline bases*

A spline function is a piecewise polynomial of order k (the polynomial degree is $k-1$ at most) defined on the interval $\Lambda =]a, b[$, whose derivatives at some order possess jump-discontinuities at breakpoints $\boldsymbol{\xi} = \{\xi_i,\ i = 1, \ldots, l+1\}$ defined by

$$a = \xi_1 < \xi_2 < \cdots < \xi_i < \cdots < \xi_l < \xi_{l+1} = b. \tag{2.1}$$

In the following, we focus on the characterization of the so-called smoothest splines, which have jump discontinuities in their $k-1$ derivative, since previous studies in Botella (1999, 2001) have assessed their superior resolving power in the collocation approach.

A spline function $\widetilde{f}(x)$ is commonly described in its B-representation

$$\widetilde{f}(x) = \sum_{i=1}^{N} \alpha_i B_i^k(x), \tag{2.2}$$

where $B_i^k(x)$ is a special spline function of order k called a B-spline which has, in particular, the property of having compact support (see *e.g.* de Boor (1978)), and the number of the B-splines is

$$N = l + k - 1. \tag{2.3}$$

The B-splines of order 1 are step functions defined by

$$B_i^1(x) = \begin{cases} 1 & \text{if } x \in [t_i, t_{i+1}[, \\ 0 & \text{otherwise,} \end{cases} \tag{2.4}$$

and an efficient construction of the B-splines of order $k \geq 2$ is given by the recurrence relation of Curry and Schoenberg (see *e.g.* de Boor (1978)):

$$B_i^k(x) = \frac{x - t_i}{t_{i+k-1} - t_i} B_i^{k-1}(x) + \frac{t_{i+k} - x}{t_{i+k} - t_{i+1}} B_{i+1}^{k-1}(x). \tag{2.5}$$

Formulae (2.4) and (2.5) introduce the knots $\{t_i,\, i = 1, \cdots, N + k\}$, which enforce the regularity of the B-spline basis by requiring

$$t_{k+i-1} = \xi_i \quad \text{for } i = 2, \cdots, l, \tag{2.6}$$

i.e the knots coincide with the breakpoints in the interior of the domain. The construction of the basis given by Eqs. (2.4)-(2.6) leaves freedom in the first k and last k of the knots. A convenient choice for the approximation of boundary value problems is to set these end-knots as

$$t_1 = \cdots = t_k = a, \quad t_{N+1} = \cdots = t_{N+k} = b. \tag{2.7}$$

In that case, by using basic properties (de Boor (1978)) such as that of compact support,

$$B_i^k(x) = 0 \quad \text{for } x \notin [t_i, t_{i+k}], \tag{2.8}$$

and partition of unity,

$$\sum_{i=1}^{N} B_i^k(x) = 1 \quad \text{for } x \in [a, b], \tag{2.9}$$

the spline function (2) satisfies

$$\widetilde{f}(a) = \alpha_1 \quad \text{and} \quad \widetilde{f}(b) = \alpha_N, \tag{2.10}$$

so that Dirichlet boundary conditions are strongly imposed. A choice analogous to (2.7) for the first k and last k knots that is suitable for imposing periodic boundary conditions is discussed in de Boor (1978) and Kravchenko *et al.* (1999).

A useful property is that a B-spline basis of order k can represent elements of the space $I\!P_k(\Lambda)$, *i.e.* polynomials of degree $k-1$ at most. More precisely, Lyche & Schumaker (1975) established the identity

$$\sum_{i=1}^{N} \gamma_{im} B_i^k(x) = x^{m-1}, \quad m = 1, 2, \ldots, k, \text{ where} \tag{2.11a}$$

$$\gamma_{im} = (-1)^{m-1} \frac{(m-1)!}{(k-1)!}\, \psi_i^{(k-m)}(0), \quad \text{with} \quad \psi_i(x) = \prod_{p=1}^{k-1} (x - t_{i+p}). \tag{2.11b}$$

In the following, the superscript referring to the order of the B-splines will be dropped for the sake of brevity.

2.2. *Semi-consistent fractional step scheme*

Numerical approximation of the Navier-Stokes equations for incompressible flows are obtained by approximating the velocity and the pressure as

$$\boldsymbol{v} = \sum_{i,j=1}^{N} \boldsymbol{v}_{i,j} B_i(x) B_j(y), \qquad p = \sum_{i,j=1}^{N-2} p_{i,j} \widetilde{B}_i(x) \widetilde{B}_j(y), \tag{2.12}$$

where $\{B_i(x), i = 1, \ldots, N\}$ and $\{\widetilde{B}_i(x), i = 1, \ldots, N-2\}$ are the compatible B-spline bases of order k introduced in Botella (1999, 2001). The Navier-Stokes equations are discretized on the collocation grid $\{(x_i, y_j);\, i, j = 1, \ldots N\}$ that will be defined later. The time-integration is based on the following prototype fractional step scheme, where the nonlinear terms are discarded,

$$\mathcal{M}\frac{\overline{U} - U^n}{\Delta t} - \mathcal{K}\overline{U} + \mathcal{M}\mathcal{M}_A^{-1}\,\widetilde{\mathcal{D}}P^n = F^{n+1}, \tag{2.13}$$

and

$$\mathcal{M}\frac{U^{n+1} - \overline{U}}{\Delta t} + \mathcal{M}\mathcal{M}_A^{-1}\widetilde{\mathcal{D}}(P^{n+1} - P^n) = 0, \tag{2.14a}$$

$$\mathcal{D}U^{n+1} = 0. \tag{2.14b}$$

In these equations, Δt is the time step, U and P are vectors representing the unknown spline coefficients of the velocity and the pressure respectively, F is a source term, $\mathcal{M}$ is the (non-diagonal) mass matrix, $\mathcal{K}$ is the viscous diffusion matrix, and $\mathcal{D}$ and $\widetilde{\mathcal{D}}$ represent first derivatives of velocity and pressure respectively. In contrast to the standard B-spline discretization considered in Botella (1999, 2001), which will be referred to as the consistent method (CM), this scheme considers a modification of the pressure gradient in Eqs. (2.13) and (2.14a) by introducing the matrix $\mathcal{M}_A^{-1}$, which is the approximate inverse of the mass matrix $\mathcal{M}$ in a sense to be defined later. The divergence equation (2.14b) is identical for both methods and expresses that the continuity condition be satisfied at the inner collocation points. Note that when $\mathcal{M}_A^{-1} = \mathcal{M}^{-1}$, the semi-consistent scheme (SCM) (2.13)-(2.14) reduces to the original CM scheme.

The main interest of the SCM scheme is that the projection step (2.14) yields the pressure equation

$$\mathcal{A}_A(P^{n+1} - P^n) = \mathcal{D}\overline{U}/\Delta t, \tag{2.15}$$

where the pressure operator

$$\mathcal{A}_A = \mathcal{D}\mathcal{M}_A^{-1}\widetilde{\mathcal{D}}, \tag{2.16}$$

is sparse when $\mathcal{M}_A^{-1}$ is sparse, resulting in a pressure equation that can be efficiently solved by standard iterative methods for elliptic problems.

The principle of scheme (2.13)-(2.14) was introduced by Gresho & Chan (1990) for the finite-element method with $\mathcal{M}_A^{-1} = \mathcal{M}_L^{-1}$, *i.e.* an approximate inverse generated by the lumped approximation which is, in general, a first-order approximation of the mass matrix. The use of a highly accurate approximate inverse is motivated by investigating the truncation error of the SCM scheme. When combining Eqs. (2.13) and (2.14a) to eliminate the provisional velocity $\overline{U}$, we get

$$\mathcal{M}\frac{U^{n+1} - U^n}{\Delta t} - \mathcal{K}U^{n+1} + \widetilde{\mathcal{D}}P^{n+1} + \mathcal{E}_S + \mathcal{E}_A = F^{n+1}, \tag{2.17}$$

where, in addition to the $O(\Delta t^2)$ splitting error

$$\mathcal{E}_S = -\Delta t\,\mathcal{K}\mathcal{M}_A^{-1}\widetilde{\mathcal{D}}(P^{n+1} - P^n), \tag{2.18}$$

common to fractional-step schemes, the approximation error

$$\mathcal{E}_A = (\mathcal{M} - \mathcal{M}_A)\mathcal{M}_A^{-1}\widetilde{\mathcal{D}}P^{n+1}, \tag{2.19}$$

is a spatial error expressing the degree of accuracy to which $\mathcal{M}_A$ approximates the consistent mass matrix $\mathcal{M}$. The use of an approximate inverse whose accuracy is consistent with the B-spline discretization is thus mandatory for preserving the accuracy of the SCM scheme.

3. Construction of approximate inverse of the mass matrix using local spline approximation

3.1. *Consistent interpolation vs. local interpolation*

The consistent interpolation of a function $f(x)$ consists in finding a spline function

$$\widetilde{f}(x) = \sum_{i=1}^{N} \alpha_i(f)\, B_i(x), \tag{3.1}$$

that takes on the values of $f(x)$ at a given set of collocation points $\{x_j,\, j = 1, \ldots, N\}$, *i.e.*

$$\sum_{i=1}^{N} \alpha_i(f)\, B_i(x_j) = f(x_j), \quad \text{for} \quad j = 1, \ldots, N. \tag{3.2}$$

This linear system takes the matrix form

$$\bar{\mathcal{M}}\boldsymbol{\alpha} = \boldsymbol{f}, \tag{3.3}$$

where $\boldsymbol{\alpha} = (\alpha_1(f), \ldots, \alpha_N(f))$, $\boldsymbol{f} = (f(x_1), \ldots, f(x_N))$ and $\bar{\mathcal{M}} = (B_i(x_j))_{i,j=1,\ldots,N}$ is the consistent, non-diagonal mass matrix of bandwidth k. The solution of a linear system of equations is thus needed for determining the spline coefficients.

In contrast, local interpolation methods were developed in *e.g.* Lyche & Schumaker (1975); de Boor (1978) such that the determination of the coefficients does not require solving a collocation system. These methods are local in the sense that the evaluation of the coefficients depends on the value of the function and/or its derivatives at a small number of data points. In the following, we focus on local schemes involving function values, *i.e.* schemes such that the i^{th} spline coefficient is determined as

$$\alpha_i(f) = \sum_{j=1}^{k_l} \beta_{ij}\, f(\tau_{ij}), \tag{3.4}$$

where $\{\tau_{ij}, j = 1, \ldots, k_l\}$ is a given set of distinct data locations in Λ, $k_l \leq k$ is the number of data points used for the evaluation of each spline coefficient and will be referred to as the order of the local scheme, and $\{\beta_{ij}, j = 1, \ldots, k_l\}$ are coefficients to be determined.

In the case where the data points are chosen from the set of collocation points, scheme (3.4) can be written in matrix form as

$$\boldsymbol{\alpha} = \bar{\mathcal{M}}_A^{-1}\boldsymbol{f}, \tag{3.5}$$

where the coefficients $\{\beta_{ij}\}$ in (3.4) define the entries of the square matrix $\bar{\mathcal{M}}_A^{-1}$ that is precisely the approximate inverse of the consistent mass matrix $\bar{\mathcal{M}}$ we are seeking. The matrix $\bar{\mathcal{M}}_A^{-1}$ is sparse, each of its row possessing k_l non-zero entries at most. Thus, the linear system solution required by the consistent approximation is now replaced by a sparse matrix-vector multiplication involving the same right-hand side.

3.2. *Derivation of the local interpolant*

The local interpolation scheme we use for the determination of the entries of $\mathcal{M}_A^{-1}$ is the scheme based on point evaluations considered in Example 3.4 of Lyche & Schumaker (1975). This construction is valid for B-spline bases of any order k and an arbitrary distribution of knots.

Given $k_\mathrm{l} \leq k$ and some data points $\{\tau_{ij}\,;\, i = 1,\dots N,\, j = 1,\dots,k_\mathrm{l}\}$ such that $\{\tau_{i1},\dots,\tau_{ik_\mathrm{l}}\}$ are distinct for all i, the coefficients $\{\beta_{ij}\,;\, i = 1,\dots,N,\, j = 1,\dots,k_\mathrm{l}\}$ in (3.4) are determined so that the local scheme reproduces polynomial of order k_l, *i.e.*

$$\widetilde{f} = f, \quad \forall f \in I\!P_{k_\mathrm{l}}(\Lambda), \quad k_\mathrm{l} \leq k. \tag{3.6}$$

For this purpose, it is convenient to write Eq. (3.4) as

$$\alpha_i(f) = \sum_{j=1}^{k_\mathrm{l}} \mu_{ij}\,[\tau_{i1},\dots,\tau_{ij}]\,f, \tag{3.7}$$

where $[\,\cdot\,,\,\cdot\,]f$ represents the divided difference of $f(x)$ (see *e.g.* de Boor (1978)). Condition (3.6) amounts to representing each monomial x^{m-1}, $m = 1,\dots,k_\mathrm{l}$, as

$$\sum_{i=1}^{N} \left(\sum_{j=1}^{k_\mathrm{l}} \mu_{ij}\,[\tau_{i1},\dots,\tau_{ij}]\,x^{m-1} \right) B_i(x) = x^{m-1}. \tag{3.8}$$

By using (2.11), the coefficients μ_{ij} are obtained as the solution of the lower triangular linear system, for each $i = 1,\dots,N$

$$\sum_{j=1}^{k_\mathrm{l}} \mu_{ij}\,[\tau_{i1},\dots,\tau_{ij}]\,x^{m-1} = \gamma_{im}, \quad \text{for} \quad m = 1,\dots,k_\mathrm{l}, \tag{3.9}$$

from which the μ_{ij} can be obtained by back-solution. The values of μ_{ij} for $j = 1,\dots,4$ are given in Lyche & Schumaker (1975) and are listed hereafter for completeness:

$$\mu_{i1} = 1, \tag{3.10a}$$

$$\mu_{i2} = \gamma_{i2} - \tau_{i1}, \tag{3.10b}$$

$$\mu_{i3} = \gamma_{i3} - (\tau_{i1} + \tau_{i2})\,\mu_{i2} - \tau_{i1}^2, \tag{3.10c}$$

$$\mu_{i4} = \gamma_{i4} - (\tau_{i1} + \tau_{i2} + \tau_{i3})\,\mu_{i3} - (\tau_{i1}^2 + \tau_{i1}\tau_{i2} + \tau_{i2}^2)\,\mu_{i2} - \tau_{i1}^3. \tag{3.10d}$$

Due to the structure of system (3.9), the values of the $\{\mu_{ij}\}$ do not depend on k_l. Thus, the coefficients of a scheme of order $k_\mathrm{l} \leq 4$ are given by the first k_l lines in Eq. (3.10). The extra effort to determine the coefficients of a scheme of order 5 would only be to calculate μ_{i5} from (3.9). Once the μ_{ij} are determined, the β_{ij} can be obtained by equating (3.7) to (3.4).

Lyche & Schumaker (1975) have shown that this local scheme yields an accuracy of order k_l in the maximum norm. In particular, for the case $k_\mathrm{l} = k$, it is thus possible to obtain a local interpolant that preserves the order of accuracy of the consistent approximation.

Another important case occurs for $k_\mathrm{l} = 2$: if, to obtain the i^{th} B-spline coefficient, the first data point τ_{i1} is chosen to be equal to $x_i^\star$ defined as

$$x_i^\star = \gamma_{i2}, \quad \text{where from (2.11}b\text{)} \quad \gamma_{i2} = \sum_{p=1}^{k-1} t_{i+p}/(k-1), \tag{3.11}$$

then $\mu_{i2} = 0$ in Eq. (3.10b) for any choice of the second data point τ_{i2}. Thus, the spline function

$$\widetilde{f}(x) = \sum_{i=1}^{N} f(x_i^\star)\, B_i(x), \tag{3.12}$$

is a second-order approximation to $f(x)$. This scheme is precisely the variation-diminishing approximation of Marsden & Schoenberg (see *e.g.* de Boor (1978)), and the collocation points (3.11) will subsequently be referred to as the Marsden-Schoenberg points.

A last important remark concerns the accuracy of the imposition of Dirichlet boundary conditions with the local scheme in the case where the end-knots are set using Eq. (2.7). From Eqs. (2.10) and (3.7), the value of the spline at the end-point $x = a$ is

$$\widetilde{f}(a) = \alpha_1(f), \quad \text{with } \alpha_1(f) = \sum_{j=1}^{k_\mathrm{l}} \mu_{1j}\,[\tau_{11}, \ldots, \tau_{1j}]\, f, \tag{3.13}$$

where the coefficients $\{\mu_{1j}, \ldots, \mu_{1k_\mathrm{l}}\}$ are solution to

$$\sum_{j=1}^{k_\mathrm{l}} \mu_{1j}\,[\tau_{11}, \ldots, \tau_{1j}]\, x^{m-1} = a^{m-1}, \quad m = 1, \ldots, k_\mathrm{l}. \tag{3.14}$$

If τ_{11} is chosen to be equal to a, the unique solution is then $\mu_{11} = 1$, $\mu_{12} = \cdots = \mu_{1k_\mathrm{l}} = 0$. From Eq. (3.13) we get $\widetilde{f}(a) = f(a)$ and, correspondingly, $\widetilde{f}(b) = f(b)$ at the other end-point, showing that Dirichlet boundary conditions are satisfied exactly just as in the consistent approximation (Eq. (2.10)).

3.3. *Approximate inverse of the mass matrix*

The local interpolant allows us to build an approximate inverse $\bar{\mathcal{M}}_A^{-1}$ of the mass matrix when the data points $\{\tau_{i,j}\}$ are chosen from the set of collocation points $\{x_i, i = 1, \ldots, N\}$. For the imposition of Dirichlet conditions with the end-knots (2.7), an additional constraint would be to set $\tau_{11} = a$ and $\tau_{N1} = b$, the choice of the remaining data points $\{\tau_{1j}\,, j = 2, \ldots, k_\mathrm{l}\}$ and $\{\tau_{Nj}\,, j = 2, \ldots, k_\mathrm{l}\}$ having no consequence.

A case of special interest arises when the approximate inverse reduces to $\bar{\mathcal{M}}_A^{-1} = \mathcal{I}$. This approximate inverse corresponds to the lumped mass matrix widely used in the finite-element community (see *e.g.* Gresho & Sani (1998)), obtained by summing the rows of the consistent mass matrix $\bar{\mathcal{M}}$ and putting the result on the diagonal. For the spline-collocation method, the local interpolant of order $k_\mathrm{l} = 1$ with $\tau_{i1} = x_i$ generates such a matrix, and thus yields first-order accuracy in general. However, as shown by the variation-diminishing scheme (3.12), the lumped mass matrix is second-order accurate when the Marsden-Schoenberg collocation points (3.11) are used.

The latter case identifies the Marsden-Schoenberg points as an alternative to the usual choice of the collocation points, *i.e.* the location of the maximum of the B-splines. These two definitions are equivalent in particular cases only, such as a periodic domain with uniform knots. They nonetheless yield the same characterization of the first and last collocation points when the end-knots (2.7) are used, namely $x_1 = a$ and $x_N = b$. In the following, the Marsden-Schoenberg points will be used as much as possible even though no advantages have yet been observed when local interpolants of order higher than 2 are employed.

As sketched in Fig. 1, the approximate inverse generated by a local scheme of order $k_\mathrm{l} \geq 3$ can be viewed as a high-order generalization of the mass lumping technique.

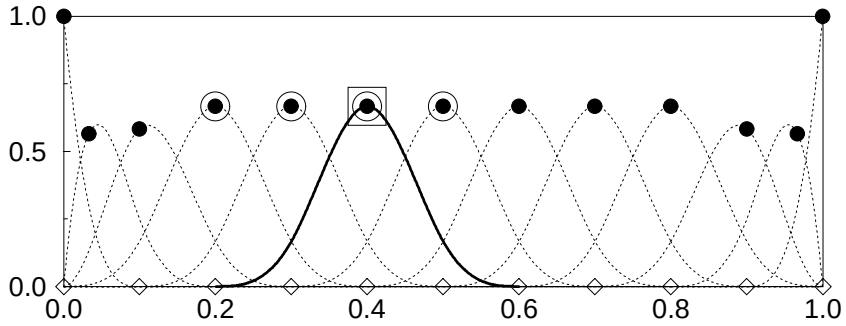

FIGURE 1. Sketch to illustrate the approximation of a function $f(x)$ with a B-spline basis of order $k = 4$, on $l+1 = 10$ equidistant breakpoints ($\diamond$) with end-knots (2.7). The coefficient associated to the 6^{th} B-spline (———) is evaluated with the values of $f(x)$ at: all Marsden-Schoenberg collocation points ($\bullet$) with the consistent approximation; a unique collocation point (framed) with the mass lumping approximation; and 4 collocation points (circled) when a local scheme of order $k_{\text{l}} = 4$ is used.

Since $\bar{\mathcal{M}}^{-1}$ is dense, the evaluation of the spline coefficient $\alpha_i(f)$ by the consistent approximation involves values of $f(x)$ at all collocation points. In contrast, the mass lumping technique consists in identifying $\alpha_i(f)$ to the value of $f(x)$ at the collocation point associated with the i^{th} B-spline. More generally, the local approximation of $\alpha_i(f)$ involves values of $f(x)$ at several collocation points, which are located in Fig. 1 in the support of $B_i(x)$. This approximation has the consequence of expanding the bandwidth of $\bar{\mathcal{M}}_A^{-1}$ while raising the accuracy of the evaluation of $\alpha_i(f)$.

Several issues have to be addressed for generating approximate inverse of practical interest. A loss in the spatial resolution power of the spline-collocation method would predictably result from the replacement of the consistent mass by the local mass approximation. Furthermore, while a $O(N^{-k_{\text{l}}})$ asymptotical accuracy is assured when k_{l} data points per coefficient are used, the definition of the local interpolant leaves freedom in their positioning. The influence of the location of the data points on the accuracy of the resulting local scheme is investigated in the next section.

4. Numerical results

4.1. *Local approximation in a one-dimensional periodic domain*

It is convenient to analyze the resolution properties of the local approximation for B-spline bases on a uniform distribution of breakpoints, with periodic boundary conditions. The investigation of the influence of the position of the data points used for generating $\bar{\mathcal{M}}_A^{-1}$ is then greatly simplified since, in this configuration, the bases are generated by translation of the same cardinal B-spline (de Boor (1978)). As a result, the i^{th} Marsden-Schoenberg point is characterized as the maximum of the spline $B_i(x)$, *i.e.* for k even

$$x_i^\star = t_{i+k/2}, \quad i = 1, \ldots, N. \tag{4.1}$$

Moreover, this configuration allows to perform the modified wavenumber analysis of the semi-consistent schemes.

The influence of the choice of the data points on the accuracy of the resulting schemes is performed for local interpolant of order $k_{\text{l}} = 4$. For completeness, results are also provide for the popular variation-diminishing scheme (*i.e.* mass lumping approximation, $k_{\text{l}} = 2$). Table 1 displays the various sets of data points that we consider. Those sets

Set of data points	Index of data points used for local interpolation	Offset of nonzero diagonals of $\mathcal{M}_A^{-1}$ with respect to the main diagonal
Set *I*	$\{ i \}$	$0,$
Set *II*	$\{ i-2,\, i-1,\, i,\, i+1 \}$	$-1,\ 0,\ 1,$
Set *II'*	$\{ i-1,\, i,\, i+1,\, i+2 \}$	$-1,\ 0,\ 1,$
Set *III*	$\{ i,\, i+1,\, i+2,\, i+3 \}$	$0,\ 1,\ 2,\ 3,$
Set *III'*	$\{ i-3,\, i-2,\, i-1,\, i \}$	$-3,\ -2,\ -1,\ 0,$
Set *IV*	$\{ i-2,\, i-1,\, i+1,\, i+2 \}$	$-2,\ -1,\ 1,\ 2,$

TABLE 1. Description of the sets of data points used for local interpolation. The index i refers to the collocation point associated with the i^{th} B-spline.

of points are located as close as possible to the support $[t_i, t_{i+k}]$ of $B_i(x)$ in order to minimize the bandwidth of $\bar{\mathcal{M}}_A^{-1}$.

Set *I* corresponds to the variation-diminishing scheme, while the five other sets use the local interpolant of order 4.

Sets *II* and *II'* represent the two possible choices of data points that yield approximate inverses with the shortest bandwidth. For the particular case of equidistant knots with periodicity conditions considered in this section, these two sets happen to generate the same symmetric tridiagonal matrix $\bar{\mathcal{M}}_A^{-1}$. In general, this property is lost when the knots are not distinct and equally spaced. As an example, for a B-spline basis on a uniform distribution of breakpoints with Dirichlet boundary conditions, the tridiagonality of $\bar{\mathcal{M}}_A^{-1}$ is lost at its first and last $k-1$ lines due to the fact that the end-knots are identical (see Eq. (2.7)).

Sets *III* and *III'* correspond respectively to a left and right biasing of the data points with respect to $x_i^\star$. It should be noted that even though these sets generate distinct approximate inverses, they yield identical results on the accuracy tests and the modified wavenumber analysis presented below. This phenomenon is understood by observing that these numerical examples do not reflect the influence of the biasing direction on the behavior of the resulting schemes.

Finally, set *IV* is designed to generate an approximate inverse, with a sparsity pattern that is symmetric on arbitrary grids, by not considering the datum at point $x_i^\star$.

The first numerical test concerns the interpolation of the periodic function

$$f(x) = \sin(10\pi x) + \cos(2\pi x + 2), \quad \text{in} \quad \Lambda =]0, 1[. \tag{4.2}$$

We recall that the consistent approximation requires a linear system solution while the semi-consistent schemes require a single sparse matrix-vector multiplication. The maximal value of the error, sampled on a fine grid of 1001 equidistant points, is displayed in Fig. 2 for splines of order $k = 4$. The poor accuracy of the lumping approximation is obvious, yielding second order accuracy. The order of accuracy of the consistent approximation is recovered for all the local schemes of order 4. These results show the importance of data point positions. Not surprisingly, the lowest error of the local schemes is obtained with set *II*. Note also that for a moderate spatial resolution ($N \leq 25$), sets *III* and *IV* yield results inferior to those obtained with the lumping approximation.

For completeness, Fig. 3 displays analogous results obtained with splines of order 6. As in the previous case, fourth-order accuracy is obtained with local schemes of order 4 and, again, set *II* displays the lowest magnitude error. The results obtained with these local

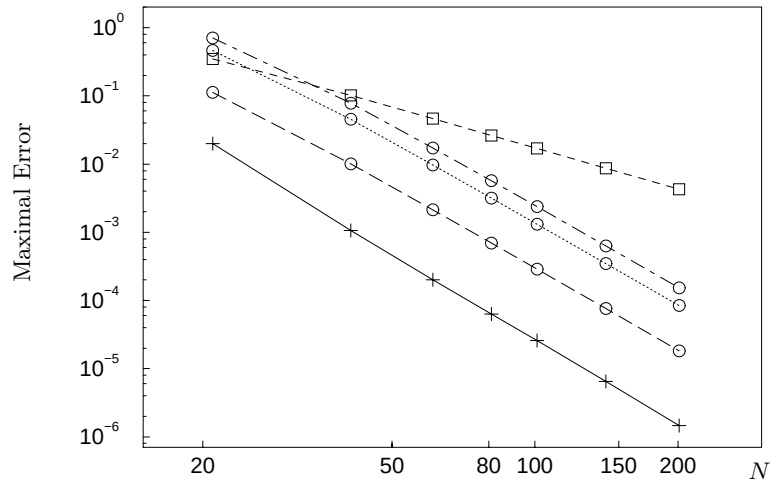

FIGURE 2. Maximal error vs. N, number of B-splines of order $k = 4$, for the various approximation methods. Local scheme with $k_1 = 2$ (□): set I – – – – ; local schemes with $k_1 = 4$ (○): set II — — — , set III ····· , set IV —·— ; consistent approximation ——— .

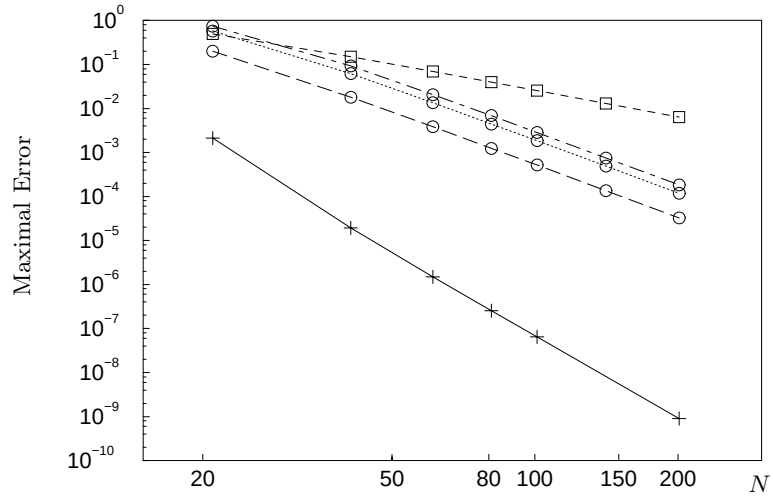

FIGURE 3. Maximal error vs. the number of points N with splines of order $k = 6$. See the caption of Fig. 2 for the labeling.

schemes are, of course, far from the 6^{th}-order accuracy of the consistent approximation. This rate of convergence would nonetheless be obtained with local schemes of order 6.

A classical evaluation of the resolving power of a scheme is given by the modified wavenumber analysis of the first derivative (*e.g.* Lele (1992)). For this purpose, the eigenvalue problem

$$u' = \lambda\, u \quad \text{in } \Lambda =]-\pi, \pi[, \tag{4.3}$$

is solved numerically with periodic boundary conditions. The complex eigenvalues with real imaginary part are denoted $\{\underline{i}\,\lambda_n,\ n = 0, \ldots, N/2\}$, the remaining ones being their

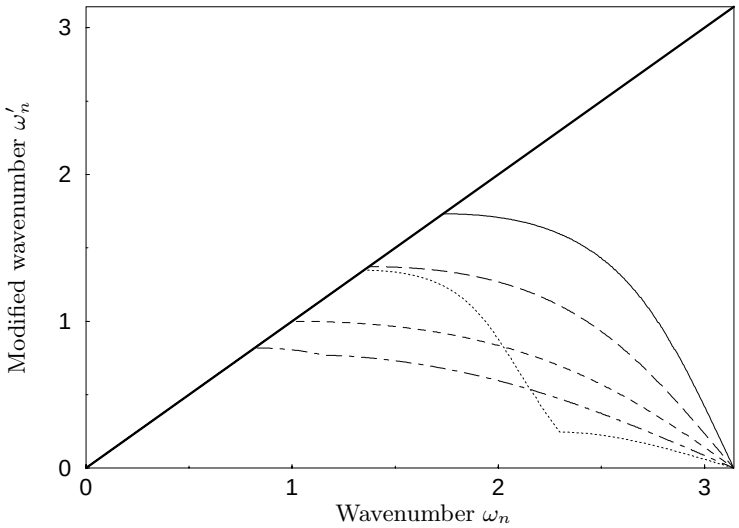

FIGURE 4. Modified wavenumber of the first derivative yielded by the different methods for splines of order $k = 4$. Local scheme with $k_l = 2$: set I – – – – ; local schemes with $k_l = 4$: set II — — — , set III ····· , set IV — · — ; consistent scheme ——— ; exact ——— .

conjugates. The discretization of (4.3) by the consistent approximation is

$$\bar{\mathcal{M}}\boldsymbol{\alpha} = \lambda\,\bar{\mathcal{D}}\boldsymbol{\alpha}, \tag{4.4}$$

where $\bar{\mathcal{D}} = (B_i'(x_j^\star))$ is the first derivative collocation operator. Correspondingly, the spectrum of the local schemes is obtained by solving

$$\boldsymbol{\alpha} = \lambda\,\bar{\mathcal{M}}_A^{-1}\bar{\mathcal{D}}\boldsymbol{\alpha}. \tag{4.5}$$

For splines of order $k = 4$ and 6 respectively, Figs. 4 and 5 sketch the modified wavenumber spectrum $\widetilde{\omega}_n = 2\pi\lambda_n/N$ versus the wavenumber $\omega_n = 2\pi n/N$ given by the different approximations. As expected, the local scheme I degrades the resolving power compared to the consistent approximation. For the local schemes of order 4, the location of the data points has a great influence on their resolving ability, yielding very disparate wavenumber plots. It is particularly striking that set IV gives lower resolving power than even the lumped mass approximation.

A more quantitative measurement of the resolving ability of a scheme is given by the resolving efficiency r_ϵ, *i.e.* the fraction of wavenumbers accurately represented within a relative tolerance of ϵ. This quantity is defined as $r_\epsilon = 2M_\epsilon/N$, where M_ϵ is the number of the modified wavenumber $\widetilde{\omega}_n$ that satisfies the error tolerance

$$\frac{|\widetilde{\omega}_n - \omega_n|}{\omega_n} \leq \epsilon, \quad n = 0, \ldots, N/2. \tag{4.6}$$

The resolving efficiency r_ϵ of the various schemes are given in Table 2 for characteristic values of ϵ. We observe that this measurement gives, once more, set II as the most accurate of the local schemes. In particular, for splines of order $k = 4$, set II recovers up to 80%, 79% and 75% of the resolved fraction r_ϵ of the consistent approximation for $\epsilon = 10^{-1}$, 10^{-2} and 10^{-3} respectively. In comparison, the lumping approximation recovers only 57%, 57% and 32% of this resolved fraction.

In summary, accurate approximate inverses that preserve the order of accuracy of the

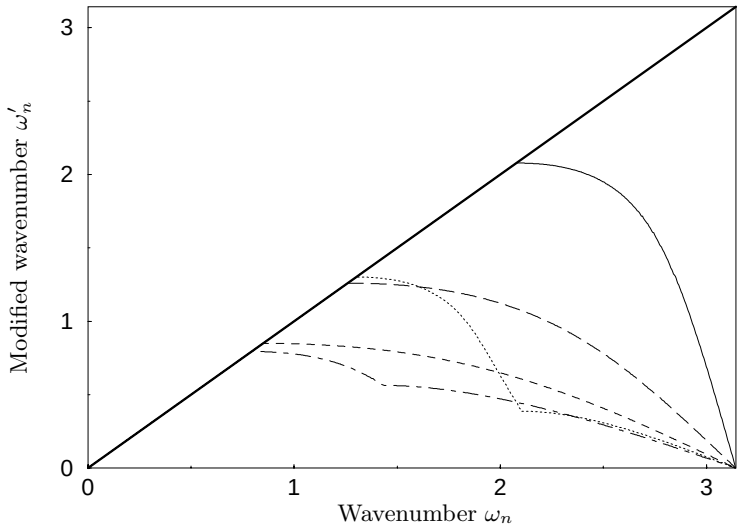

FIGURE 5. Modified wavenumber of the first derivative for splines of order $k = 6$. See the caption of Fig. 4 for the labeling.

Schemes	Order $k = 4$			Order $k = 6$		
	$\epsilon = 0.1$	$\epsilon = 0.01$	$\epsilon = 0.001$	$\epsilon = 0.1$	$\epsilon = 0.01$	$\epsilon = 0.001$
Consistent	0.61	0.56	0.44	0.73	0.67	0.61
Set *I*	0.36	0.32	0.14	0.30	0.27	0.16
Set *II*	0.49	0.44	0.33	0.45	0.41	0.30
Set *III*	0.48	0.43	0.28	0.46	0.42	0.26
Set *IV*	0.29	0.27	0.20	0.28	0.26	0.19

TABLE 2. Resolving efficiency r_ϵ of the first derivative for the various approximations with $N/2 = 750$.

consistent approximation can be generated when a sufficient number of data points is used. The location of these data points is nonetheless of crucial importance. These numerical tests have found the best position of these data points on a periodic uniform grid to be set *II*. The resolution properties of the consistent approximation are, nonetheless, not fully recovered by the local schemes. The marginal loss in accuracy is greatly counterbalanced by their much lower computational cost, as it will be illustrated in the next section.

In the case of Dirichlet boundary conditions, set *II* is used as a template for building approximate inverses of order $k_\mathrm{l} = 4$ on a uniform distribution of breakpoints. The local approximation of coefficients with indices $i = k, \ldots, N-k+1$ is performed with this set, generating a centered tridiagonal approximation as in the periodic case. A modification has to be performed for the first and last $k-1$ deficient B-splines, *i.e.* which display multiple knots in their support. The first and last coefficients use the datum at the endpoint a and b respectively, leading to the exact imposition of the Dirichlet conditions. For the remaining B-spline coefficients with indices $i = 2, \ldots, k-1$ and $i = N-k, \ldots, N-1$, we use the collocation points with indices $\{i-1, i, i+1, i+2\}$ and $\{i-2, i-1, i, i+1\}$ respectively.

4.2. *Semi-consistent approximation of the Div-Grad problem*

We are now ready to describe the semi-consistent approximation (SCM) of the projection step (2.14) by considering as model equations the Div-Grad problem:

$$\sigma\,\boldsymbol{v} + \nabla p = \mathbf{f} \quad \text{in } \Omega =]0,1[^2, \tag{4.7a}$$

$$\nabla \cdot \boldsymbol{v} = 0 \quad \text{in } \Omega =]0,1[^2, \tag{4.7b}$$

$$\boldsymbol{v} = \mathbf{g} \quad \text{on } \partial\Omega. \tag{4.7c}$$

This new discretization follows essentially along the lines of the consistent method (CM) introduced in Botella (1999, 2001). Eqs. (4.7a) and (4.7b) are evaluated on the $(N-2)\times(N-2)$ inner collocation points, while the remaining boundary points are used for the determination of the boundary conditions (4.7c). The discretization of the divergence equation (4.7b) is identical for both methods and reads in matrix form:

$$\mathcal{D}U = G, \tag{4.8}$$

where the velocity coefficients determined from the boundary conditions are put in the right-hand side (RHS).

The SCM approximation of Eq. (4.7a) is now described with some details related to the imposition of non-homogeneous boundary conditions. For this purpose, we denote by $\mathcal{I}_I$ the set of indices of collocation points in the interior of domain, and, correspondingly, $\mathcal{I}_B$ refers to the indices of the boundary nodes. The discretization of Eq. (4.7a) at the interior collocation point (x_i, y_k) is

$$\sigma \sum_{(j,l)\,\in\,\mathcal{I}_I} \mathcal{M}^A_{i,k,j,l}\, U_{j,l} + \sum_{(j,l)\,\in\,\mathcal{I}_I} \widetilde{d}_{i,k,j,l} P_{j,l} = F_{i,k}\ , \tag{4.9a}$$

where $\{\widetilde{d}_{i,k,j,l}\}$ are the gradient coefficients of the pressure spline, and

$$F_{i,k} = \mathbf{f}(x_i, y_k) - \sigma \sum_{(j,l)\,\in\,\mathcal{I}_B} \mathcal{M}^A_{i,k,j,l}\, U_{j,l}\ , \tag{4.9b}$$

corresponds to a RHS augmented with boundary velocity coefficients. The matrix form of (4.9a) reads

$$\sigma U + \mathcal{M}_A^{-1}\widetilde{\mathcal{D}} P = \mathcal{M}_A^{-1} F, \tag{4.10}$$

where $\mathcal{M}_A^{-1}$ is constructed from the tensor product of one-dimensional matrices $\bar{\mathcal{M}}_A^{-1}$ in each spatial direction, which use the distribution of data points for Dirichlet conditions described in the previous section.

On the other hand, the entries $\{\mathcal{M}^A_{i,k,j,l}\}$ in Eq. (4.9b) need to be determined for the imposition of the boundary conditions. For this purpose, the sum in (4.9b) is expanded as

$$\sum_{(j,l)\,\in\,\mathcal{I}_B} \mathcal{M}^A_{i,k,j,l}\, U_{j,l} = \sum_{(j,l)\,\in\,\mathcal{I}_B} \bar{\mathcal{M}}^A_{i,j}\, \bar{\mathcal{M}}^A_{k,l}\, U_{j,l}\ , \tag{4.11}$$

by using tensor product properties. For $j = 1, \ldots, N$, the coefficients $\{\bar{\mathcal{M}}^A_{i,j}\,;\, i = 2, \ldots, N-1\}$ in the $x-$direction are then obtained by solving the one-dimensional problems

$$\bar{\mathcal{M}}_A^{-1}\boldsymbol{x}^j = \boldsymbol{\delta}^j, \qquad \text{with } \boldsymbol{\delta}^j = (\delta_{j,m}\,;\, m = 1, \ldots, N), \tag{4.12}$$

giving as solution $\boldsymbol{x}^j = (\bar{\mathcal{M}}^A_{i,j}\,;\, i = 1, \ldots, N)$. An analogous procedure is performed for determining the coefficients in the $y-$direction.

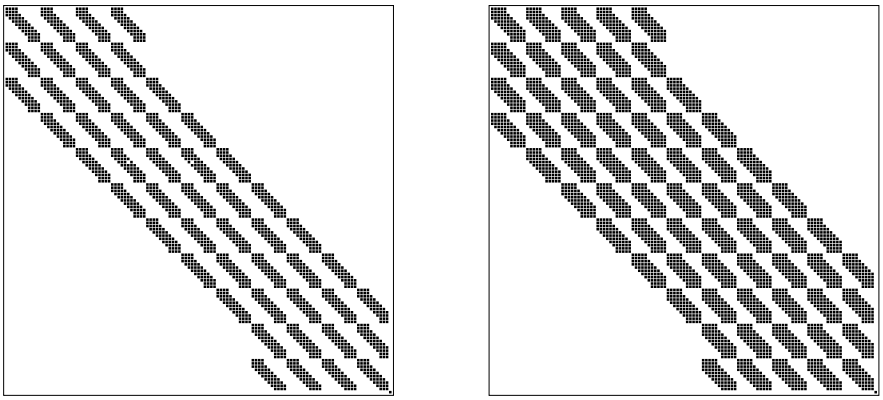

FIGURE 6. Sparsity pattern of $\mathcal{A}_A$ on a 13×13 uniform grid for splines of order $k = 4$, generated with the mass lumping approximation (left) and the approximate inverse of order 4 (right).

Equations (4.8) and (4.10) yield the pressure equation

$$\frac{1}{\sigma}\mathcal{A}_A P = \frac{1}{\sigma}\mathcal{D}\mathcal{M}_A^{-1}F - G, \tag{4.13a}$$

where the pressure operator

$$\mathcal{A}_A = \mathcal{D}\mathcal{M}_A^{-1}\widetilde{\mathcal{D}}, \tag{4.13b}$$

is constructed by multiplication of sparse matrices. These operations are performed with the SPARSKIT package (Saad (1990)).

Raising the order of the approximate inverse increases the number of non-zero entries of $\mathcal{A}_A$. In two dimensions, when a natural ordering of the unknowns is used, a modification of the block structure of $\mathcal{A}_A$ is observed. As an illustration, Fig. 6 compares the structure of pressure operators generated by the lumping approximation and the approximate inverse of order 4. These operators have a similar block-structured pattern where the 11×11 blocks are more or less filled according to the order of the approximate inverse. For splines of order 4, we observe that an approximate inverse of order 4 doubles the number of non-zero entries of the pressure operator compared to the lumped mass approximation. Correspondingly, an increase of 70% of the entries is observed for splines of order 6.

The semi-consistent method is now evaluated against the consistent method by numerically solving problem (4.7) with $\sigma = 1$, for the solution

$$\boldsymbol{v} = \mathbf{rot} \sin 4\pi x \sin 4\pi y, \quad p = \cos 4\pi x \cos 4\pi y,$$

on a uniform distribution of knots. For comparison with results obtained in Botella (1999, 2001), the collocation points are set as the location of the maximum of the velocity B-splines. The maximum error on the first-component of the velocity u and the pressure, sampled on a 300×300 uniform grid, is reported in Fig. 7. For splines of order 4 (Fig. 7(a)), the use of an approximate inverse of order 4 maintains the order of accuracy of the consistent approximation, namely $O(N^{-4})$ for u and $O(N^{-2})$ for p. It is striking to observe that the magnitude of the error on p is almost identical for both schemes, while the velocity errors of the SCM scheme are only marginally higher. The latter is certainly the consequence of the inferior resolving power of the semi-consistent approximation that we observed in Section 4.1. As it would be expected, the 6^{th}-order accuracy on u displayed in Fig. 7(b) by the CM scheme with splines of order 6 is not recovered by the

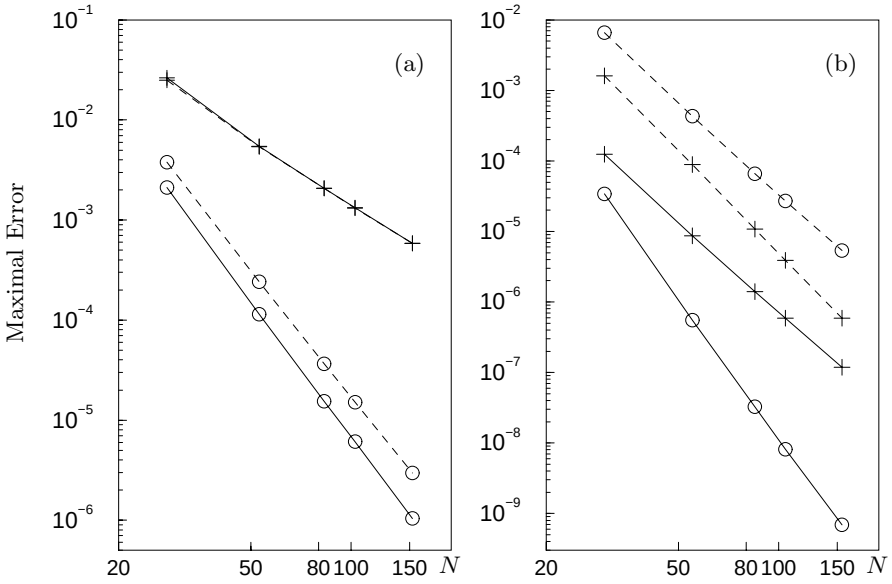

FIGURE 7. Solution of the Div-Grad problem with (a) splines of order 4, and (b) splines of order 6. Maximum error on u o——o , p +——+ , CM approximation; maximum error on u o– – –o , p +– – –+ , SCM approximation with approximate inverse of order 4.

approximate inverse of order 4, and a fourth-order convergence rate is observed in this case.

It is valuable to compare the CPU cost required by the iterative solution of the CM and SCM equations. To give a fair evaluation, both systems are solved by similar iterative techniques with the error tolerance (*i.e.* the l^2 norm of the discrete divergence (4.8)) set to $\epsilon = 10^{-8}$.

Since the pressure operator of the CM discretization is dense and thus cannot be stored, the equations are solved by the Uzawa algorithm developed in Botella (1999, 2001), which is accelerated by the Bi-CGSTAB method (see *e.g.* Saad (1996)). The preconditioner of this system is $\mathcal{A}_L = \mathcal{D}\mathcal{M}_L^{-1}\widetilde{\mathcal{D}}$, *i.e.* an SCM pressure operator where the lumping approximation is used. The use of this preconditioner has the effect of making the number of Uzawa iterations independent from the mesh size. Each step of the Uzawa algorithm requires inversions of the consistent mass matrix and the preconditioner. These problems are respectively solved by a direct method and the Bi-CGSTAB algorithm with ILU(m) preconditioning. The value $m = 0$ is used for splines of order 4 and $m = 2$ for splines of order 6, and the error tolerance is set to 10^{-10}.

The SCM system precludes the use of Uzawa iterations, resulting in a far less cumbersome solution procedure. The pressure equation (4.13) is solved with the same Bi-CGSTAB algorithm used for inverting the preconditioner $\mathcal{A}_L$ of the CM system. The velocity is then recovered by using Eq. (4.10).

Table 3 reports the CPU time observed for solving these systems on a sequence of increasingly fine grids. The savings in CPU time yielded by the SCM method are tremendous: for splines of order $k = 4$ the CPU cost is divided by 30, while this ratio reaches 100 for $k = 6$. Intuitively, these savings can be understood when observing that the computational cost of the solution of the SCM pressure equation is roughly equivalent to a single inversion of the preconditioner of the CM solution procedure. The ratio of savings

Splines of order $k = 4$				Splines of order $k = 6$			
N	SCM	CM	Ratio	N	SCM	CM	Ratio
28	0.06	2.57	42.8	30	0.05	5.53	110.6
53	0.46	14.76	32.1	55	0.29	26.52	91.4
83	1.88	60.80	32.3	85	1.11	131.63	118.6
153	12.32	399.34	32.4	105	1.98	211.71	106.9

TABLE 3. Comparison of CPU time (in seconds) observed for the solution various approximation of the Div-Grad problem.

is thus proportional to the number of Uzawa iterations required for convergence. Since the number of Uzawa iterations is independent of the grid size but increases with the order of the B-splines, the SCM solution method becomes more attractive as the order of the discretization is raised.

5. Conclusion and future plans

Preliminary results on the application of the SCM scheme to the solution of the Navier-Stokes equations have been obtained. These important tests assess *(a)* the high spatial accuracy of the Navier-Stokes solver and *(b)* its robustness for unsteady computations. The time-integration is based on scheme (2.13)-(2.14), with second-order backward-differentiation of the time-derivative and Adams-Bashforth discretization of the nonlinear term. This fractional step scheme yields second-order time accuracy for both velocity and pressure (Botella (1999, 2001)). In order to obtain a fourth-order spatially accurate method, B-splines of order $k = 6$ are used in each direction, with the approximate inverse of order $k_{\text{l}} = 4$.

The first test concerns the validation of the spatial accuracy of the SCM scheme on a uniform grid. For this purpose, we consider the steady solution

$$\boldsymbol{v} = \mathbf{rot} \sin \pi x \sin \pi y, \quad p = \frac{1}{4}(\cos 2\pi x \cos 2\pi y) + 10(x + y),$$

in the domain $\Omega =]-1, 1[^2$. Fig. 8 displays the normalized l^2 errors obtained when the steady-state is reached. This figure confirms that the method is indeed fourth-order accurate for both velocity and pressure.

The second test illustrates the accuracy and stability of the method for computing unsteady solutions. We consider the computation of the periodic flow in the regularized driven cavity flow at $Re = 12,000$, taking as a reference the spectral computation of Shen (1991) performed with 65 Chebyshev polynomials in each direction and the time step $\Delta t = 5 \times 10^{-3}$. For comparison purpose, the SCM computation uses the same discretization parameters with a similar grid refined near the boundary by a Chebyshev distribution of knots. The initial condition is defined as the steady flow at $Re = 10,000$. Fig. 9 displays the time-evolution of the kinetic energy on nearly half a million time-steps. The periodic state is asymptotically reached with the same period $T = 3.085 \pm \Delta t$ measured by Shen (1991). This result shows the ability of the SCM method to conserve kinetic energy on a long time integration and to reproduce spectral results with a similar coarse spatial resolution.

The use of highly accurate approximate inverse in association to the SCM scheme led to the development of a Navier-Stokes solver that preserves the accuracy of the B-spline

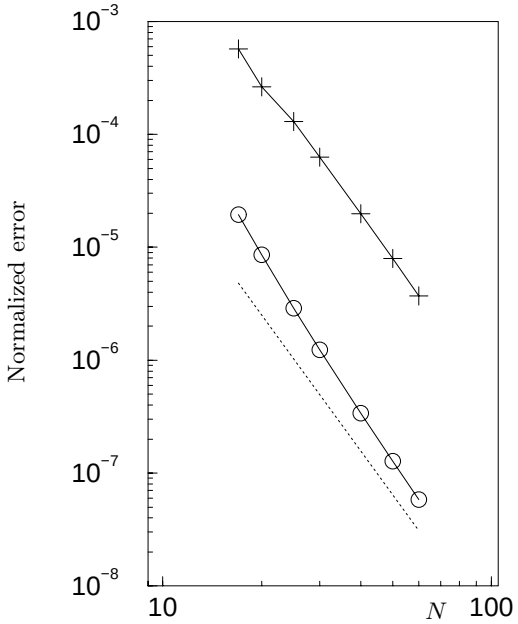

FIGURE 8. Spatial error on u (o——o) and p (+——+) obtained on the steady state solution of the Navier-Stokes equations; ····· : reference line of slope -4.

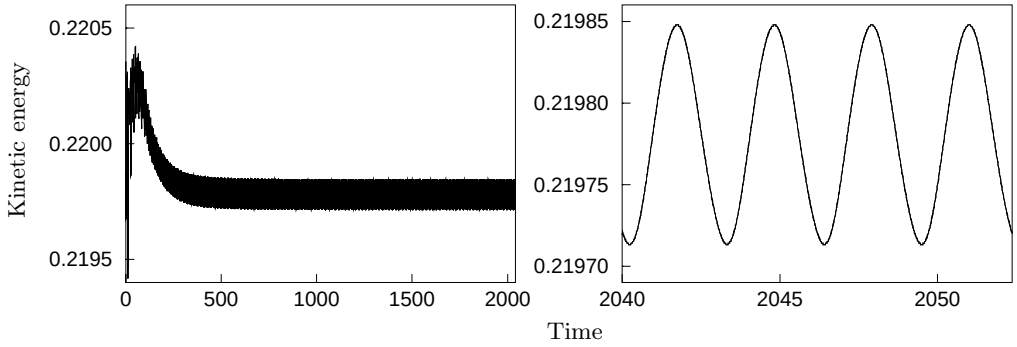

FIGURE 9. Time evolution of the kinetic energy in the driven cavity at $Re = 12000$ computed by the SCM fractional-step scheme on a 65×65 grid with $\Delta t = 5 \times 10^{-3}$.

in a cost-effective way. The high computational interest of the fractional step method is indeed recovered: the full decoupling of the velocity and pressure allows the solution to sparse elliptic problems only at each time-cycle.

This solver would serve as the building block for performing highly-accurate LES simulations of complex flow on semi-structured meshes. The solver is currently updated for the handling of more general geometries, the flow past a circular cylinder being considered as a first application. The semi-structured multidimensional approximations will be constructed by using the mesh embedding algorithm of Shariff & Moser (1998). Several issues related to the extension of the tensor product B-spline approximation have to be addressed. The algorithm should be modified to generate in a compatible fashion the semi-structured staggered bases of the velocity and pressure. In addition, the construction of approximate inverse has to be extended to the case of these multidimensional B-splines.

Acknowledgments

The author is grateful to Dr. K. Shariff for valuable discussions during the course of this work.

REFERENCES

de Boor, C. 1978 *A Practical Guide to Splines.* Springer.

Botella, O. 1999 A velocity-pressure Navier-Stokes solver using a B-spline collocation method. *Annual Research Briefs*, Center for Turbulence Research, NASA Ames/Stanford Univ. 403-421.

Botella, O. 2001 On a collocation B-spline method for the solution of the Navier-Stokes equations. *Computers & Fluids*, to be published.

Christara, C. C. & Smith, B. 1997 Multigrid and multilevel methods for quadratic spline collocation. *BIT.* **37**(4), 781-803.

Gresho, P. M. & Chan, S. T. 1990 On the theory of semi-implicit projection methods for viscous incompressible flow and its implementation via a finite element method that also introduces a nearly consistent mass matrix. Part 1: Theory & Part 2: Implementation. *Int. J. Numer. Methods Fluids.* **11**, 587-620 & 621-659.

Gresho, P. M., Lee, R. L. & Sani, R. L. 1978 Advection-dominated flows, with emphasis on the consequence of mass lumping. *Finite Elements in Fluids,* J. Wiley & Sons. **3**, 335-350.

Gresho, P. M. & Sani, R. L. 1998 *Incompressible Flow and the Finite Element Method.* J. Wiley & Sons.

Harlow, F. H. & Welch, J. 1965 Numerical calculation of time-dependent viscous incompressible flow of fluid with free surfaces. *Phys. Fluids.* **8**, 2181-2189.

Kravchenko, A. G. & Moin, P. 1997 On the effect of numerical errors in large eddy simulations of turbulent flows. *J. Comput. Phys.* **131**, 310-322.

Kravchenko, A. G. & Moin, P. 2000 Numerical studies of flow over a circular cylinder at $Re_D > 3900$. *Physics Fluids.* **12**, 403-417.

Kravchenko, A. G., Moin, P. & Shariff, K. R. 1999 B-spline method and zonal grids for simulation of complex turbulent flows. *J. Comput. Phys.* **151**, 757-789.

Lele, S. K. 1992 Compact finite difference schemes with spectral-like resolution. *J. Comput. Phys.* **103**, 16-42.

Lyche, T. & Schumaker, L. L. 1975 Local spline approximation methods. *J. Approx. Theory.* **15**, 294-325.

Nicoud, F., Baggett, J. S., Moin, P. & Cabot, W. 2001 LES wall modeling based on optimal control theory. *Phys. Fluids,* to be published.

Saad, Y. 1990 SPARSKIT: A basic tool kit for sparse matrix computations. *Tech. Rep. 90-20.* Research Institute for Advanced Computer Science, NASA Ames Research Center, Moffett Field, CA.

Saad, Y. 1996 *Iterative Methods for Sparse Linear Systems.* PWS.

Shariff, K. & Moser, R. D. 1998 Two-dimensional mesh embedding for B-spline methods. *J. Comput. Phys.* **145**, 471-488.

Shen, J. 1991 Hopf bifurcation of the unsteady regularized driven cavity flow. *J. Comput. Phys.* **95**, 228-245.

Vasilyev, O. V. 2000 High order finite difference schemes on non-uniform meshes with good conservation properties. *J. Comput. Phys.* **157**, 746-761.